5-2006

Modulation of Fast and Slow Inactivation in Two Cardiac NAv Channel Isoforms by SDZ 211-939

Tyce Jeffrey Kearl
Utah State University

MODULATION OF FAST AND SLOW INACTIVATION IN TWO CARDIAC NA_V CHANNEL ISOFORMS BY SDZ 211-939

by

Tyce Jeffrey Kearl

Thesis submitted in partial fulfillment
of the requirements for the degree

of

HONORS IN UNIVERSITY STUDIES
WITH DEPARTMENT HONORS

in

Biology

Approved:

Thesis/Project Advisor	Department Honors Advisor
Peter Ruben, Ph.D.	*Kim Sullivan, Ph.D.*

Director of Honors Program

Christie Fox, Ph.D.

UTAH STATE UNIVERSITY
Logan, UT

2006

Bachelor's Thesis

Tyce J. Kearl

Department of Biology, Utah State University, Logan, Utah 84322, USA

Modulation of fast and slow inactivation in two cardiac Na_v channel isoforms by SDZ 211-939

Abstract

Here we report a hitherto unknown effect of a synthetic inactivation inhibitor on inactivation in cardiac sodium channels ($Na_v1.5$) from two different species: human and bovine. SDZ 211-939 stabilized the slow inactivated-state in both channels as seen by an increased steady-state probability of slow inactivation. SDZ also destabilized the fast-inactivated state and increased the amplitude of persistent currents. SDZ modulated conductance parameters, open-state fast inactivation time constants, and activation kinetics of $hNa_v1.5$, but not $bNa_v1.5$. These findings will aid future studies designed to elucidate the binding site and molecular mechanisms of inactivation inhibitors such as SDZ 211-939.

1. Introduction

Cardiac voltage-gated sodium channels ($Na_v1.5$) are responsible for the influx of ionic current that initiates myocardial action potentials. From the membrane resting potential, depolarization causes the channel to go from a closed (deactivated) state to an open (activated) state. Channels inactivate through two distinct mechanisms: fast and slow inactivation. Membrane excitability, and therefore action potentials, is regulated by the likelihood of a channel being in an inactivated state. The type of inactivation, fast or slow, differentially regulates membrane excitability. Cellular modification of both types of inactivation allows excitable membrane activity to be controlled. Such modification also suggests a convenient method of pharmacological intervention in diseased and/or mutant cells.

The importance of properly functioning inactivation may be seen by the conditions associated with abnormal inactivation activity. Fast [1,2] and slow inactivation [3] in $Na_V1.5$ have both been shown to cause life-threatening arrhythmias such as Brugada syndrome and chromosome 3-linked congenital long-QT syndrome. Another factor pointing to the importance of slow inactivation regulation in $Na_v1.5$ is the drastic reduction of slow inactivation in cardiac channels compared to skeletal channels. Approximately 20% of cardiac channels are slow-inactivated in steady-state protocols [4] versus 80% in skeletal muscle channels [5]. If cardiac channels were slow-inactivated to the same extent as in the skeletal muscle isoform, myocardial tissue would quickly cease to conduct action potentials.

Fast inactivation occurs rapidly via structural components on the intracellular side of the sodium channel [6], with onset and recovery time constants on the order of milliseconds. Slow inactivation, however, has time constants on the order of seconds and is homologous with

cumulative inactivation [7]. Whereas fast inactivation-kinetics allow membrane excitability to be regulated over the course of an action potential, slow inactivation requires sustained or repeated depolarizations for its effects to become physiologically relevant. Interestingly, the two states are "reciprocally interactive" [8], the probability of one having an inverse relationship with that of the other [6,9,10].

SDZ 211-939 (SDZ) belongs to a family of membrane permeable synthetic inactivation inhibitors typified by DPI 201-106 (DPI) [11]. SDZ acts as a positive inotropic agent by prolonging the open-state of $Na_v1.5$ channels through inhibition of fast inactivation [12]. The prolonged time spent in the open-state lengthens the duration of the action potential and increases the intracellular Na^+ concentration. This lessens the concentration gradient driving the Na^+/Ca^{2+}-exchanger and results in a stronger force of contraction in myocardial tissue due to increased intracellular Ca^{2+}-availability to contractile proteins [13]. Because of increased contractility, DPI and other synthetic modifiers have been clinically studied to determine their therapeutic usefulness in cases of cardiac failure [14,15,16].

Neither the binding site nor the mechanism of action for this family of compounds has been identified. Researchers found [17], cloned, and characterized via heterologous expression [12] a bovine cardiac sodium channel with drastically reduced sensitivity to DPI and its derivative SDZ. The bovine cardiac channel ($bNa_v1.5$) is 92% homologous to the human cardiac channel ($hNa_v1.5$). Both the amount of similarity between the two channels and the unique effect of SDZ on the bovine channel make these two channels well suited to studies seeking to determine the mechanism and binding site of this family of inactivation inhibitors.

The main focus of our study was to ascertain the amount (if any) by which SDZ affects the steady-state probability of slow inactivation in cardiac channels. Since the probability of a

channel being in the slow-inactivated state is a determinant of myocardial excitability modulation of slow inactivation presents a convenient way by which cell excitability may be pharmacologically altered. In general, we sought in this study to characterize and compare the effects of SDZ on $hNa_v1.5$ and $bNa_v1.5$ in an effort to better understand the structure/function relationship of $Na_v1.5$.

2. Materials and Methods

2.1. Cell Culture

The cDNA for the α-subunit of either $hNa_v1.5$ or $bNa_v1.5$ (subcloned into pRc/CMV vector, Invitrogen, Carlsbad, CA) was transfected into a human embryonic kidney cell line (HEK293, ATCC number CRL-1573) using Polyfect Transfection Reagent (Qiagen, Valencia, CA). The cDNA for either the CD8 antigen or EGFP (subcloned into pEGFP-C1vector, Clontech, Palo Alto, CA) was co-transfected in some experiments to aid with identification by Dynabeads (M-450 CD8, Dynal, Oslo, Norway) or fluorescence. 24-36 hours after transfection and 24 hours before patch clamping, cells were plated onto glass cover slips. Cells were maintained at 37°C in a humidified atmosphere with 5% CO_2.

2.2. Electrophysiology

Sodium currents were recorded using the whole-cell patch clamp technique. All recordings were done in a chamber containing (in mM): NaCl 140, KCl 4, $CaCl_2$ 2, $MgCl_2$ 1, HEPES 10, pH 7.4. After fabrication (P-57, Sutter Instruments, Novato, CA), borosilicate patch electrodes were coated with dental wax to reduce capacitance. Electrode resistance in the bath

solution prior to attachment to the cell was between 1 and 3 MΩ. Prior to recordings, the electrodes were thermally polished and filled with (in mM): CsCl 130, NaCl 10, EGTA 10, Mg-ATP 4, Li-GTP 0.4, HEPES 10, pH 7.4. Temperature was maintained at 22± 0.2°C by a Peltier device regulated by a temperature controller (HCC-100A, Dagan, Minneapolis, MN). Data were obtained with an EPC-9 amplifier (HEKA, Lambrecht, Germany) and were software-low-pass-filtered at 5 kHz. Sampling frequency was 50 kHz for slow inactivation protocols and 200 kHz for all *I/V* protocols. Pulse software (HEKA) run on a G4 Macintosh was used to control both voltage clamping and pulse protocols. After formation of a ≥1 giga-Ohm seal, the seal was allowed to stabilize for 30 s. A patch of membrane was excised via intra-electrode suction to allow for whole-cell access. No recordings were done until peak current elicited by test pulses remained steady (approximately two minutes). Leak subtraction was performed automatically by a p/4 procedure before each pulse protocol. Fast and series resistance were automatically compensated such that series resistance was <10 MΩ. Holding potential was maintained at –100 mV between pulse protocols. Data sets with current rundown of greater than 10% were discarded.

Steady-state slow inactivation data were obtained from the following pulse protocol. Membrane potential was held at –130 mV for 20 s to recover channels from previously induced slow inactivation. A 60 s prepulse ranging from –130 to –10 mV was then delivered. Prepulse potentials were alternated between high and low sweeps (–130, –10, –120, –20, etc.) to avoid accumulation of slow inactivation during the experiment. After the prepulse, the channels recovered from fast inactivation during a 20 ms pulse at –130 mV before a test pulse of 20 ms at –10 mV.

Conductance data were obtained as follows. Membrane potential was held at –130 mV for 200 ms to insure that the channels were deactivated, stepped to a test pulse voltage (–90 to 40 mV in 10 mV increments) for 20 ms, and then returned to –130 mV for the next sweep. The test pulse voltage was sufficiently long to observe activating and fast-inactivating sodium current.

After collection of control data, two mL of 2.5 or 25 μM SDZ (from where?, dissolved in DMSO) were perfused into the recording chamber. SDZ data were not obtained during the two minutes after perfusion, to allow for diffusion of SDZ and its association with the channels.

2.3. Data Analysis

Data were analyzed in PulseFit (HEKA) and IgorPro (Wavemetrics, Lake Oswego, OR) software. Steady-state slow inactivation curves were obtained from normalized data averaged and fitted with the modified Boltzmann equation:

$$I/I_{max} = (I_1 - I_2)/[1 + \exp(-ze_0(V_m - V_{1/2}))/(kT)] + I_2 \quad (1)$$

where I_{max} is the maximum peak current measured, I_1 and I_2 are respectively the maximum and minimum values fitted, z is the apparent valence (slope factor), e_0 is the elementary charge, V_m is the prepulse potential, $V_{1/2}$ is the midpoint potential, k is the Boltzmann constant, and T is the absolute temperature. The maximum probability of steady-state slow inactivation was reported as I/I_{max} at the most depolarized voltage of the curve and will be referred to as 'probability of slow inactivation'.

Conductance data were obtained from I/V curves using the equation:

$$G = I_{max}/(V_m - E_{rev}) \quad (2)$$

where G is conductance, E_{rev} is the reversal potential derived from minimizing error in G, and other variables as stated above. Normalized conductance curves were then averaged and fitted with the modified Boltzmann equation:

$$I / I_{maz} = I_1/[1 + \exp(-ze_0(V_m - V_{1/2}))/(kT)] \quad (3)$$

where the variables are the same as those for equation 1 with the exception of V_m being the test pulse potential.

Open-state fast inactivation time constants were obtained by fitting the current decay portion of the I/V curves to the single exponential equation:

$$I(t) = I_p + a_1 \exp(-t/\tau) \quad (4)$$

where $I(t)$ is current amplitude as a function of t (time), I_p is the plateau amplitude, a_1 is the amplitude at $t = 0$ (time of peak current), and τ is the time constant.

$I_{plateau}$:I_{peak} ratios were analyzed as follows: I_{peak} (peak current amplitude) was fit with a 6th order polynomial function. $I_{plateau}$ (plateau current amplitude) was derived by fitting the sustained current amplitude with a horizontal line. The sustained current amplitude was defined by the current after 15-20 ms of the 20 ms test pulse; by 15 ms, current amplitudes in all experiments had reached a plateau and remained steady to the end of the test pulse.

$I_{plateau}$:I_{peak} ratios and fast inactivation time constants were graphed using Excel (Microsoft, Redmond, WA). All other graphs were made in IgorPro.

All statistical values were obtained using the Student's t-test, or, when indicated by a significant difference is standard deviations, Welch's alternate t-test using Instat software (GraphPad Software, Inc., San Diego, CA). Two-tailed p-values are reported. Significant difference was accepted at $p<0.05$. Statistical values are given as mean ± standard error of the mean (SEM). Throughout the text, n refers to the number of experiments.

3. Results

3.1. SDZ affects plateau current in $hNa_v1.5$ and $bNa_v1.5$

The primary effect of synthetic inactivation inhibitors, such as SDZ appears to be to destabilize the fast-inactivated state and thus create a plateau (or persistent) current. A greater amount of destabilization results in an increased plateau current.

To determine the effect of SDZ on plateau (or persistent) current, we measured the $I_{plateau}$:I_{peak} ratio at the end of a depolarizing test pulse. A 20 ms test pulse to –10 mV elicited currents after a conditioning pulse at –130 mV for 200 ms. This protocol was sufficiently long to display both peak and plateau currents.

As shown in Figure 1, $hNa_v1.5$ and $bNa_v1.5$ had similar $I_{plateau}$:I_{peak} ratios in the absence of SDZ ($p< 0.57$). Application of 2.5 μM and 25 μM SDZ resulted in a concentration-dependent increase of $I_{plateau}$:I_{peak} ratios for both channel isoforms, although there was virtually no difference in response to SDZ between the two isoforms.

3.2. SDZ modulates open-state fast inactivation time constants and activation kinetics of $hNa_v1.5$ but not $bNa_v1.5$

Open-state fast inactivation time constants are illustrated in Figure 2 for voltages at which large sodium currents were observed (–20 mV to 40 mV). Although SDZ affected $bNa_v1.5$ by either increasing (25 μM) or decreasing (2.5 μM) the time constants, the effect was not

significant at either concentration. For $hNa_v1.5$, however, a significant increase was seen at the voltages 0, 10, 20, and 30 mV following the perfusion of 25 μM SDZ.

Activation kinetics (data not shown) were obtained by measuring the current rise time (defined as the rising portion of the current trace between 10% and 90% of the peak current amplitude) during test pulses to –10 mV.

2.5 μM SDZ significantly decreased the activation time constants (dT) of $hNa_v1.5$ from 397 ± 26 μs (15) to 301 ± 22 μs (10) ($p< 0.02$). The application of 25 μM SDZ to $hNa_v1.5$ slightly increased dT to 435 ± 50 μs (15); however, the increase in dT was not statistically significant ($p< 0.51$). The dT of $bNa_v1.5$ followed the same trends as $hNa_v1.5$ in that 2.5 μM SDZ decreased dT from 378 ± 26 μs (18) to 314 ± 40 μs (6) and 25 μM SDZ increased dT to 438 ± 34 μs (6). These changes in dT were not statistically significant, ($p <0.22$ and 0.18, respectively).

3.3. SDZ differentially modulates conductance parameters

The most visible example of differential modulation by SDZ is seen by the effect of the compound on the voltage-dependence of the channels (see conductance curves in Figure 3). SDZ caused large, significant shifts to more hyperpolarized potentials in $hNa_v1.5$, whereas such shifts in activation voltage-dependence were not seen for $bNa_v1.5$.

The midpoint potential ($V_{1/2}$) of $hNa_v1.5$ was shifted -22.0 mV by 2.5 μM SDZ ($p< 0.0001$). No additional increase in this effect was seen at the higher concentration of SDZ (25 μM) where $V_{1/2}$ was shifted-13.6 mV ($p< 0.003$). The effect on $V_{1/2}$ was not concentration-dependent in isoforms from both species as the effects on $V_{1/2}$ by the two concentrations were

not significantly different ($p< 0.051$). Additionally, the control $V_{1/2}$ measurements from each isoform were very different with $bNa_v1.5$ having a $V_{1/2}$ 28.9 mV more hyperpolarized than $hNa_v1.5$.

3.4. SDZ increases the steady-state probability of slow inactivation of $hNa_v1.5$ and $bNa_v1.5$

Previous studies using SDZ did not examine its effects on slow inactivation. Due to the large effect of SDZ on fast inactivation [12] and the coupling between fast and slow inactivation [5], we sought to determine the extent to which SDZ might affect the probability of slow inactivation in $Na_v1.5$. The channel isoforms $hNa_v1.5$ and $bNa_v1.5$ were used for two reasons. First, slow inactivation parameters of $hNa_v1.5$ have been previously studied and abnormal slow inactivation function implicated in several medical conditions [22,23]. Second, $bNa_v1.5$ has been shown to be minimally affected by SDZ compared to this channel isoform in other species [12,17]; differential effects between the two isoforms might thus reveal important information about the mechanisms and structures underlying the effects of SDZ.

Figure 4 shows the steady-state slow inactivation curves for both channel types. The maximum probability of slow inactivation for both hNav1.5 and $bNa_v1.5$ was significantly increased by application of 25 μM SDZ ($p< 0.0003$ and $p< 0.04$, respectively). Data showing the effect of SDZ on the midpoint ($V_{1/2}$) and the apparent valence (z) were also measured and are summarized in Table 1. Interestingly, although SDZ affected the probability of slow inactivation, no significant effects were observed for $V_{1/2}$, and the apparent valence was affected by SDZ only in $bNa_v1.5$ ($p< 0.01$).

4. Discussion

Our data demonstrate that, besides the well-studied effect of synthetic modifiers such as DPI on the stability of fast inactivation [18,19,20], one member of this class of drugs, SDZ, also affects the stability and probability of slow inactivation. We have additionally shown that SDZ differentially modulates the conductance parameters and open-state fast inactivation time constants $hNa_v1.5$ and $bNa_v1.5$.

Single channel recordings show that fast-inactivated channels undergo "bursting" during prolonged depolarizations. Bursting activity occurs when channels briefly recover from fast inactivation, allowing conductance of sodium current as the channels are in the activated open-state, and then re-enter the fast-inactivated open-state [21]. The $I_{plateau}$:I_{peak} ratios we observed are likely due to bursting channels. Bursting activity represents the relative stability of the fast inactivated-state; bursting increases as the stability of the fast-inactivated state decreases. Because our pulse protocols ensured nearly complete fast inactivation (verified by control data), the SDZ-induced increase in $I_{plateau}$:I_{peak} ratio represents a decrease in stability of the fast inactivated-state. For our control experiments, $I_{plateau}$ values are two orders of magnitude smaller than I_{peak}. With the addition of 25 μM SDZ, $I_{plateau}$ values increased by an order of magnitude compared to I_{peak}.

Understanding SDZ modulation of slow inactivation is difficult since the underlying mechanisms by which channels slow inactivate are poorly understood [22,23]. However, several studies have shown an inverse relationship between the probabilities of fast and slow inactivation [4,9,10]. Given our results showing a decrease of fast inactivation stability and an increase of

slow inactivation stability, it appears that SDZ may exert its effects on the two types of inactivation via their intrinsic coupling.

Previous studies have shown 1) that of swine, goat, and cattle, only cattle exhibited reduced sensitivity to SDZ [17], and 2) that SDZ is markedly less effective in $bNa_v1.5$ compared to $rNa_v1.5$ [12]. Based on these studies we hypothesized that the primary effect of SDZ, inactivation inhibition, on $hNa_v1.5$ would be more similar to $rNa_v1.5$ than $bNa_v1.5$ (which had been the only identified channel with reduced sensitivity to SDZ). Our plateau current results show that SDZ destabilizes inactivation in $hNa_v1.5$ and $bNa_v1.5$ to the same extent and contradict the hypothesis. However, Denac *et al.* (2002) expressed $bNa_v1.5$ and $rNa_v1.5$ in *Xenopus* oocytes, whereas we expressed our channels in HEK293 cells. Different expression systems have been shown to affect the biophysical properties of sodium channels and it is possible that the inactivation destabilization effect of SDZ is altered by the expression system [24].

The main area of structural difference between $bNa_v1.5$ and other channel-isoforms lies in the cytoplasmic linker connecting domains II and III. Although the bovine and human isoforms have DII-DIII linkers of the same length, the amount of conserved primary sequence in only 82% in the DII-DIII linker compared with 92% for the entire sequence. Interestingly, mutations found in the human DII-DIII linker have effects similar to those of SDZ on persistent currents although the wildtype sequence at these amino acids is conserved between the bovine and human isoform. The polymorphism S1103Y has been correlated with an increased risk of cardiac arrhythmias and was identified in 13.2% of African-Americans [25] and in a white family [26]. A997S, associated with Sudden Infant Death Syndrome, also displays increased $I_{plateau}$ [27].

The bovine amino acid residue corresponding to position 1103 in $hNa_v1.5$ is conserved, but the residue corresponding to position 997 in $hNa_v1.5$ is not conserved. The residue at this position (1002) is serine, corresponding to the $I_{plateau}$-altering human polymorphism A997S. However, this does not imply that a serine at the position universally increases $I_{plateau}$ or is involved in SDZ binding. In addition to demostrating similar $I_{plateau}$:I_{peak} ratio responses to SDZ when compared with $hNa_v1.5$, bnav1.5 still displays the low level of $I_{plateau}$ characteristic of wild-type cardiac channels and not the increased level observed for A997S [27]. Further studies are needed to elucidate the role of that position on inactivation stability.

The mechanism by which SDZ affects sodium channels is unclear. Considering the increased plateau current amplitudes in S1103Y and A997S, and $hNa_v1.5$ + SDZ compared to the wild-type isoform, it appears that SDZ might destabilize fast inactivation by inducing a conformational change. These factors also lead to the hypotheses that the DII-DIII linker is involved in fast-inactivation stability, and that the linker may be the binding site for SDZ and related compounds. Whether SDZ modulates slow inactivation directly or via a fast-slow inactivation coupling remains to be determined. The DII-DIII linker has not, however, been previously associated with the control of slow inactivation, suggesting an indirect effect of SDZ on slow inactivation. Thus, the stabilization of slow inactivation, as suggested by the increase in its maximum probability (Fig. 4), may be an indirect consequence of the destabilization of fast inactivation, as suggested by the increase in time constants of $hNa_v1.5$ (Fig. 2) and the increase in persistent current in both isoforms (Fig. 1).

In summary, we have shown that SDZ differentially affects $hNa_v1.5$ and $bNa_v1.5$, and that an inactivation inhibitor not only modulated fast inactivation but also the probability of slow inactivation. These results may serve as a basis for future studies aimed at elucidating the

molecular mechanism of SDZ and the structure/function relationships of sodium channels. Importantly, an understanding of the molecular mechanisms of both inactivation inhibitors and sodium channel activity will aid the rational design of novel drugs for chronic cardiac failure, a possibility that has not been adequately explored [16,12]. In light of recent studies showing the expression of "neuronal" sodium channel isoforms in the heart [28,29], it will also be important to study the effects of SDZ on these isoforms to gain a complete understanding of the compound's effects on cardiac function.

Acknowledgements

This work was supported by an American Heart Association grant (to Peter C. Ruben) and a Utah State University U.R.C.O. grant (to T.J.K.). The author wishes to thank fellow laboratory members for technical and editorial assistance and Drs. Peter C. Ruben and Meike Mevissen for the mentorship and assistance.

Table 1 Slow Inactivation, Conductance, and $I_{plateau}$:I_{peak} data

channel	SDZ application	*slow inactivation*			*conductance*		$I_{plateau}$:I_{peak}
		level (%)	apparent valence (z)	$V_{1/2}$ (mV)	apparent valence (z)	$V_{1/2}$ (mV)	
$hNa_v1.5$	none (control)	70 ± 2 (8)	-2.5 + 0.2 (8)	-80.9 ± 2.1 (8)	3.3 ± 0.3 (15)	-18.5 ± 2.0 (15)	0.042 ± 0.012 (15)
	2.5 μM SDZ	—	—	—	4.6 ± 0.5 (10)[a]	-40.5 ± 1.8 (10)[a]	0.120 ± 0.024 (10)[a]
	25 μM SDZ	85 ± 2 (7)[a]	-2.5 ± 0.2 (7)	-77.4 ± 4.0 (7)	4.3 ± 0.5 (15)	-32.1 ± 3.6 (15)[a]	0.496 ± 0.046 (15)[a]
$bNa_v1.5$	none (control)	78 + 3 (5)	-3.6 ± 0.2 (5)[a]	-91.0 ± 4.7 (5)[a]	3.5 ± 0.3 (18)	-47.4 ± 3.1 (18)[a]	0.034 ± 0.008 (18)
	2.5 μM SDZ	—	—	—	3.1 ± 0.2 (6)	-50.3 ± 4.6 (6)	0.093 ± 0.021 (6)[b]
	25 μM SDZ	88 ± 1 (4)[b]	-2.5 ± 0.2 (4)[b]	-83.9 ± 2.6 (4)	4.5 ± 0.5 (9)	-48.2 ± 2.4 (9)	0.449 ± 0.073 (9)[b]

All slow inactivation and conductance values were obtained from Boltzmann fits to individual data sets (as described in Materials and Methods). Data are presented as means ± SEM (n). [a]$P < 0.05$ versus $hNa_v1.5$ control. [b]$P < 0.05$ versus $bNa_v1.5$ control.

Fig. 1. A. Sodium current traces showing the effect of SDZ on plateau current and an illustration of the pulse protocol used to obtain $I_{plateau}$:I_{peak} ratios and conductance data (presented in Table 1). **B.** Graph and table of $I_{plateau}$:I_{peak} ratios for $hNa_v1.5$ and $bNa_v1.5$ with and without SDZ. Obtained from the protocol described in Figure 2. [a]$I_{plateau}$:I_{peak} ratios of $hNa_v1.5$ significantly increased with 2.5 and 25 μM SDZ ($p< 0.004$, 0.0001). [b]$I_{plateau}$:I_{peak} ratios of $bNa_v1.5$ increased similarly upon application of 2.5 and 25 μM SDZ ($p< 0.004$, 0.0005).

Fig. 2. The time constant of fast inactivation in $hNa_v1.5$ is differentially affected by SDZ. Panel A shows the time constants of fast inactivation, derived from an exponential function fit to the decay of current during a test pulse to the voltages shown on the X-axis, in $hNa_v1.5$ in the absence (light gray circles) and presence of SDZ (2.5 μM; dark gray triangles, and 25 μM; black squares). Panel B shows the time constants of fast inactivation in $bNa_v1.5$ in the absence (light gray circles) and presence of SDZ (2.5 μM; dark gray triangles, and 25 μM; black squares).

Fig. 3. A. Conductance curves (obtained from the protocol illustrated in Fig. 1) for $hNa_v1.5$ (light gray), $hNa_v1.5$ + 2.5 μM SDZ (medium gray), and $hNa_v1.5$ + 25 μM SDZ (black). **B.** Conductance curves for $bNa_v1.5$ (light gray), $bNa_v1.5$ + 2.5 μM SDZ (medium gray), and $bNa_v1.5$ + 25 μM SDZ (black). Conductance curves shown above were fitted with a modified Boltzmann equation (see Materials and Methods). [a]$P < 0.05$ versus $hNa_v1.5$ control midpoint. [b]$P < 0.05$ versus $hNa_v1.5$ apparent valence. No

significant differences were seen for SDZ-perfused $bNa_v1.5$ compared to $bNa_v1.5$ control.

Fig. 4. Average steady-state slow inactivation curves fitted with a modified Boltzmann equation. **A.** Curves for $hNa_v1.5$ (light gray) and $hNa_v1.5$ + 25 μM SDZ (black). **B.** Curves for $bNa_v1.5$ (light gray) and $bNa_v1.5$ + 25 μM SDZ (black). Inset shows pulse protocol (see Materials and Methods for details). Data were not gathered for 2.5 μM SDZ.

Figure 1

A

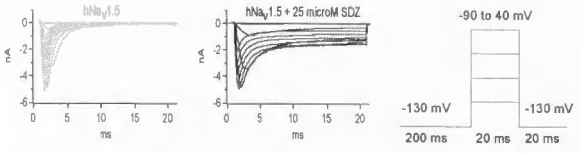
hNav1.5
hNav1.5 + 25 microM SDZ
nA
ms
-90 to 40 mV
-130 mV
-130 mV
200 ms
20 ms
20 ms

B

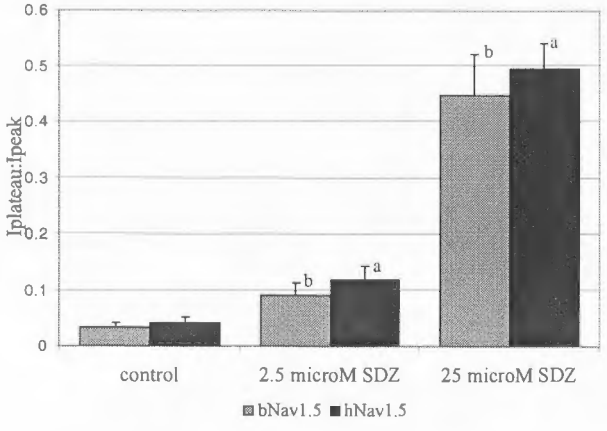
Iplateau:Ipeak
0.6
0.5
0.4
0.3
0.2
0.1
0
b
a
b
a
control
2.5 microM SDZ
25 microM SDZ
bNav1.5
hNav1.5

Figure 2

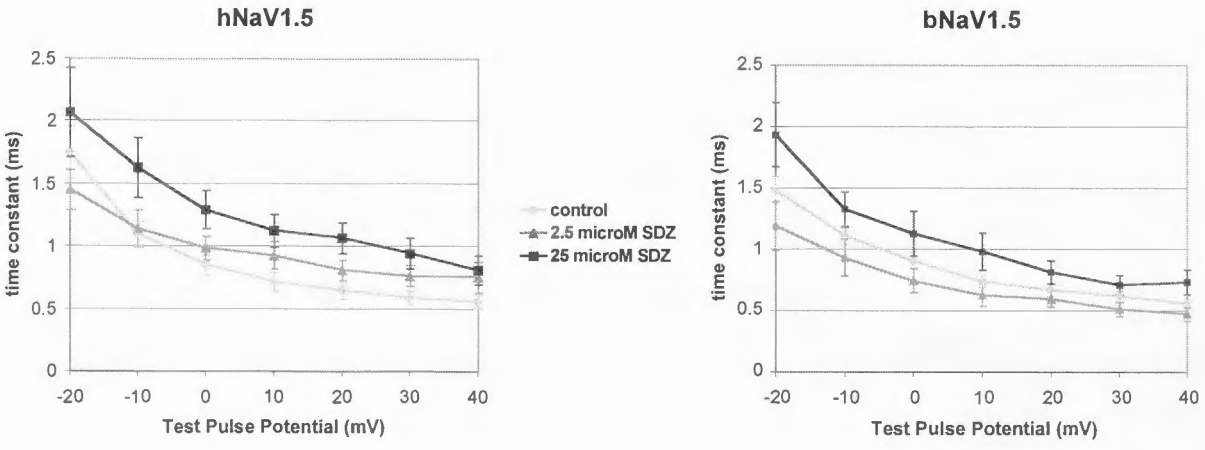
hNaV1.5
time constant (ms)
2.5
2
1.5
1
0.5
0
-20
-10
0
10
20
30
40
Test Pulse Potential (mV)
control
2.5 microM SDZ
25 microM SDZ
bNaV1.5
time constant (ms)
2.5
2
1.5
1
0.5
0
-20
-10
0
10
20
30
40
Test Pulse Potential (mV)

Figure 3

A

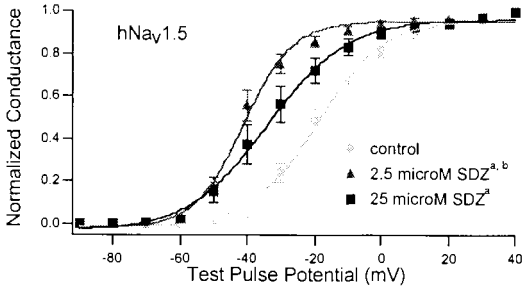
hNa$_V$1.5
Normalized Conductance
1.0
0.8
0.6
0.4
0.2
0.0
-80
-60
-40
-20
0
20
40
Test Pulse Potential (mV)
control
2.5 microM SDZ[a, b]
25 microM SDZ[a]

B

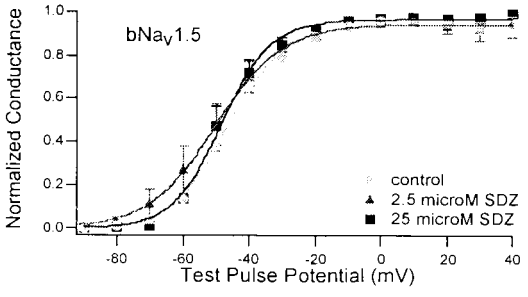
bNa$_V$1.5
Normalized Conductance
1.0
0.8
0.6
0.4
0.2
0.0
-80
-60
-40
-20
0
20
40
Test Pulse Potential (mV)
control
2.5 microM SDZ
25 microM SDZ

Figure 4

A

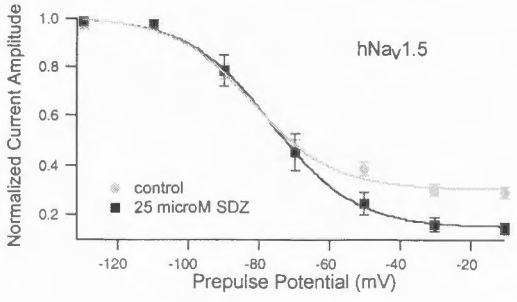
Normalized Current Amplitude
1.0
0.8
0.6
0.4
0.2
hNaV1.5
control
25 microM SDZ
-120
-100
-80
-60
-40
-20
Prepulse Potential (mV)

B

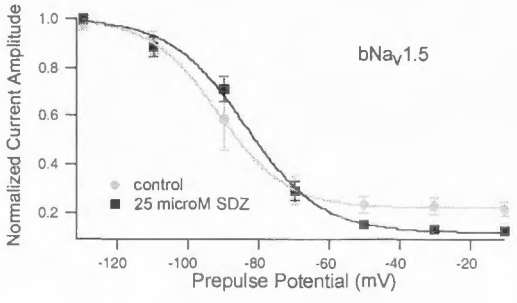
Normalized Current Amplitude
1.0
0.8
0.6
0.4
0.2
bNaV1.5
control
25 microM SDZ
-120
-100
-80
-60
-40
-20
Prepulse Potential (mV)

C

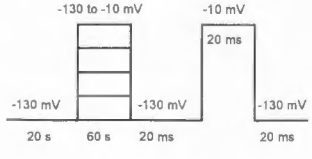
-130 to -10 mV
-10 mV
20 ms
-130 mV
-130 mV
-130 mV
20 s
60 s
20 ms
20 ms

References

[1] Bennett PB, Yazawa K, Naomasa M, George AL. Molecular mechanism for an inherited cardiac arrhythmia. Nature 1995; 376:683–5.

[2] Dumaine R, Towgin JA, Brugada P, Vatta M, Nesterenko DV, Nesterenko VV, et al. Ionic mechanisms responsible for the electrocardiographic phenotype of the Brugada syndrome are temperature dependent. Circ Res 1999; 85:803–9.

[3] Veldkamp MW, Viswanathan PC, Bezzina C, Baartscheer A, Wilde AAM, Balser JR. Two distinct congenital arrhythmias evoked by a multidysfunctional Na+ channel. Circ Res 2000; 86:e91-7.

[4] Richmond JE, Featherstone DE, Hartmann HA, Ruben PC. Slow inactivation in human cardiac sodium channels. Biophys J 1998; 74(6):2945-52.

[5] Featherstone DE, Richmond JE, Ruben PC. Interaction between fast and slow inactivation in Skm1 sodium channels. Biophys J 1996; 71:3098-109.

[6] West JW, Patton DE, Scheuer T, Wang Y, Goldin AL, Catterall WA. A cluster of hydrophobic amino acid residues required for fast Na^+-channel inactivation. PNAS 1992; 89:10910-14.

[7] Struyk AF, Cannon SC. Slow inactivation does not block the aqueous accessibility to the outer pore of voltage-gated Na channels. J Gen Physiol 2002; 120:509-16.

[8] McCollum IJ, Vilin YY, Spackman E, Fujimoto E, Ruben PC. Negatively charged residues adjacent to IFM motif in the DIII-DIV linker of hNa(V)1.4 differentially affect slow inactivation. FEBS Lett 2003; 552(2-3):163-9.

[9] Nuss BH, Balser JR, Orias DW, Lawrence JH, Tomaselli GF, Marban E. Coupling between fast and slow inactivation revealed by analysis of a point mutation (F1304Q) in μ1 rat skeletal muscle sodium channels. J Physiol 1996; 494(2):411-29.

[10] Kontis KJ, Goldin AL. Sodium channel inactivation is altered by substitution of voltage sensor positive charges. J Gen Physiol 1997; 110:403-13.

[11] Scholtysik G, Salzmann R, Quast U, Berthold R, Ott H, Schaad A, et al. SDZ 2311-939, a new cardiotonic Na^+ current activator. Naunyn Schmiedebergs Arch Pharmacol 1993; 347:345.

[12] Denac H, Mevissen M, Kuhn FJ, Kuhn C, Guionaud CT, Scholtysik G, et al. Molecular cloning and functional characterization of a unique mammalian cardiac Na(v) channel isoform with low sensitivity to the synthetic inactivation inhibitor (-)-(S)-6-amino-alpha-[(4-diphenylmethyl-1-piperazinyl)-methyl]-9H-purine-9-ethanol (SDZ 211-939). J Pharmacol Exp Ther 2002; 303(1):89-98.

[13] Scholtysik G. Cardiac Na+ channel activation as a positive inotropic principle. J Cardiovasc Pharmacol 1989; 14(S3):S24-9.

[14] Kostis JB, Lacy CR, Raia JJ, Dworkin JH, Warner RG, Casazza LA. DPI 201-106 for severe congestive heart failure. Am J Cardiol 1987; 60(16):1334-9.

[15] Bohm M, Diet F, Kemkes B, Wankerl M, Erdmann E. Inotropic response to DPI 201-106 in the failing human heart. Br J Pharmacol 1989; 98(1):275-83.

[16] Flesch M, Erdmann E. Na+ channel activators as positive inotropic agents for the treatment of chronic heart failure. Cardiovasc Drugs Ther 2001; 15(5):379-86.

[17] Mevissen M, Denac H, Schaad A, Portier CJ, Scholtysik G. Identification of a cardiac sodium channel insensitive to synthetic modulators. J Cardiovasc Pharmacol Ther 2001; 6(2):201-12.

[18] Krafte DS, Davison K, Dugrenier N, Estep K, Josef K, Barchi RL, et al. Pharmacological modulation of human cardiac Na+ channels. Eur J Pharmacol 1994; 266(3):245-54.

[19] Yuill KH, Convery MK, Dooley PC, Doggrell SA, Hancox JC. Effects of BDF 9198 on action potentials and ionic currents from guinea-pig isolated ventricular myocytes. Br J Pharmacol 2000; 130(8):1753-66.

[20] Kohlhardt M, Frobe U, Herzig JW. Modification of single cardiac Na+ channels by DPI 201-106. J Membr Biol 1986; 89(2):163-72.

[21] Clancy CE, Tateyama M, Kass RS. Insights into the molecular mechanisms of bradycardia-triggered arrhythmias in long QT-3 syndrome. J Clin Invest 2002; 110(9):1251-62.

[22] Goldin AL. Mechanisms of sodium channel inactivation. Curr Opin Neurobiol 2003; 13(3):284-90.

[23] Vilin YY, Ruben PC. Slow inactivation in voltage-gated sodium channels: molecular substrates and contributions to channelopathies. Cell Biochem Biophys 2001; 35(2):171-90.

[24] Wang DW, George AL, Bennet PB. Comparison of Heterologously Expressed Human Cardiac and Skeletal Muscle Sodium Channels. Biophys J 1996; 70:238-45.

[25] Splawski I, Timothy KW, Tateyama M, Clancy CE, Malhotra A, Beggs AH, et al. Variant of SCN5A sodium channel implicated in risk of cardiac arrhythmia. Science 2002; 297:1333-6.

[26] Chen S, Chung MK, Martin D, Rozich R, Tchou PJ, Wang Q. SNP S1103Y in the cardiac sodium channel gene SCN5A is associated with cardiac arrhythmias and sudden death in a white family. J Med Genet 2002; 39:913-5.

[27] Ackerman MJ, Siu BL, Sturner WQ, Tester DJ, Valdivia CR, Makielski JC, et al. Postmortem molecular analysis of SCN5A defects in Sudden Infant Death Syndrome. JAMA 2001; 286(18):2264-69.

[28] Maier SKG, Westenbroek RE, Yamanushi TT, Dobrzynski H, Boyett MR, Catterall WA, et al. An unexpected requirement for brain-type sodium channels for control of heart rate in the mouse sinoatrial node. PNAS 2003; 100(6):3507–12.

[29] Lei M, Jones SA, Liu J, Lancaster MK, Fung SS, Dobrzynski H, et al. Requirement of neuronal- and cardiac-type sodium channels for murine sinoatrial node pacemaking. J Physiol 2004; 559(3):835-48.